

MeV-mass dark matter and primordial nucleosynthesis

Pasquale D. Serpico and Georg G. Raffelt

Max-Planck-Institut für Physik (Werner-Heisenberg-Institut), Föhringer Ring 6, 80805 München, Germany

(Dated: 27 May 2004)

The annihilation of new dark matter candidates with masses m_X in the MeV range may account for the galactic positrons that are required to explain the 511 keV γ -ray flux from the galactic bulge. We study the impact of MeV-mass thermal relic particles on the primordial synthesis of ^2H , ^4He , and ^7Li . If the new particles are in thermal equilibrium with neutrinos during the nucleosynthesis epoch they increase the helium mass fraction for $m_X \lesssim 10$ MeV and are thus disfavored. If they couple primarily to the electromagnetic plasma they can have the opposite effect of lowering both helium and deuterium. For $m_X = 4$ –10 MeV they can even improve the overall agreement between the predicted and observed ^2H and ^4He abundances.

PACS numbers: 95.35.+d, 26.35.+c, 14.80.-j

I. INTRODUCTION

In a recent series of papers the intriguing possibility was explored that the cosmic dark matter consists of new elementary particles with masses in the MeV range [1, 2, 3, 4, 5]. While weakly interacting massive particles (WIMPs) as dark matter candidates, notably supersymmetric particles, are usually thought to have masses exceeding tens of GeV, it is not difficult to come up with viable MeV-mass candidates such as sterile neutrinos [6] or axinos [7]. The remarkable aspect of the MeV candidates studied in Refs. [1, 2, 3, 4, 5] is that they are taken to be *thermal* relics and thus require a primordial annihilation rate much larger than given by ordinary weak interactions. Contrary to naive intuition, such particles are not excluded by any obvious laboratory measurement or astrophysical argument [1, 2, 3, 4, 5, 8]. Quite on the contrary, it was argued that the annihilation of these dark matter particles in the galactic bulge can produce enough positrons to explain the 511 keV γ -ray signature that was recently confirmed by the INTEGRAL satellite [9, 10] and that seems difficult to explain with traditional astrophysical sources. Alternatively, decaying low-mass dark matter particles have also been proposed as a positron source [11, 12].

In the early universe, weak interactions freeze out at a temperature of about 1 MeV, just before the epoch of big-bang nucleosynthesis (BBN). Therefore, MeV-mass particles with larger-than-weak interaction rates are expected to be in thermal equilibrium at BBN and thus would add to the primordial energy density and expansion rate. One naively expects such particles to increase the primordial helium mass fraction Y_p , exacerbating the tension between observations and the BBN prediction. This expectation bears out for new particles coupling primarily to neutrinos. However, the new particles proposed in Refs. [1, 2, 3, 4, 5] would primarily interact with the electromagnetic plasma. It turns out that the BBN effects of these particles are non-trivial and certainly disfavor masses below about 2 MeV, but masses in the approximate range 4–10 MeV actually have the opposite effect of *lowering* Y_p without significantly af-

fecting deuterium. Therefore, the concordance between the predicted and observed ^4He and ^2H abundances is slightly improved. This little-known but intriguing effect was found a long time ago in a general study of the impact of new particles on BBN [13]. The main purpose of our work is to re-examine this effect in the context of the MeV-mass dark matter hypothesis and with the help of a modern BBN calculation and current observational data.

In addition to our BBN study presented in Sec. II we briefly consider two other possible consequences of MeV-mass dark matter particles. In Sec. III we note that the same mechanism proposed to explain the γ -ray signature from the galactic bulge should also produce a diffuse background of low-energy cosmic-ray positrons in the solar neighborhood. This argument strengthens the conclusion reached independently in Refs. [1, 2, 3, 4, 5] that an s-wave annihilation cross section for the reaction $X\bar{X} \rightarrow e^+e^-$ is strongly disfavored. Further, in Sec. IV we consider possible energy-transfer effects caused by such particles trapped in the Sun or other stars. These effects turn out to be very small because the trapping efficiency is inhibited by the smallness of m_X . In Sec. V we summarize our conclusions.

II. MEV-MASS PARTICLES AND BIG-BANG NUCLEOSYNTHESIS

A. Impact of New Particles

Thermal relic particles freeze out at a cosmic temperature T_F that for weakly interacting particles is about 1 MeV. If the particle mass is somewhat larger than T_F the number density is suppressed by annihilations so that the relic density is maximal for m_X of order T_F , i.e. for neutrinos the relic mass density would be maximal for MeV-range masses and overclose the universe by about five orders of magnitude [14]. Therefore, MeV-mass thermal relics must interact far more strongly than neutrinos so that they annihilate more efficiently to reduce their density to a level compatible with the dark-matter abun-

dance. We briefly summarize the relationship between the annihilation cross section and the relic density in Appendix A. The result reveals that MeV-mass dark matter particles must have been in thermal equilibrium throughout most of the primordial nucleosynthesis epoch so that the exact final dark-matter abundance is not relevant for our study. We will use the equilibrium assumption in our numerical implementation that was performed by a modified version of the new BBNCODE recently developed in Naples and documented in Ref. [15].

The impact of our new particles on BBN differs qualitatively and quantitatively depending on the dominant annihilation and scattering channels. Before turning to specific cases we discuss how the BBN equations and inputs are affected. To this end we first note that the new particles enter BBN through the second Friedmann equation $H^2 = (8\pi/3)G_N \rho_{\text{tot}}$ by their contribution to the total mass-energy density ρ_{tot} . We consider the X -particles to be in perfect thermal equilibrium and assume that the number densities of particles and antiparticles are the same for those cases where $X \neq \bar{X}$. The number density, pressure, and energy density contributed by the new particles is thus taken to be

$$\begin{aligned} n_X &= \frac{g_X}{2\pi^2} T_X^3 \int_x^\infty dy \frac{y(y^2 - x^2)^{1/2}}{e^y \pm 1}, \\ P_X &= \frac{g_X}{6\pi^2} T_X^4 \int_x^\infty dy \frac{(y^2 - x^2)^{3/2}}{e^y \pm 1}, \\ \rho_X &= \frac{g_X}{2\pi^2} T_X^4 \int_x^\infty dy \frac{y^2(y^2 - x^2)^{1/2}}{e^y \pm 1}, \end{aligned} \quad (1)$$

where $x = m_X/T_X$ and the sign $+$ ($-$) refers to fermion (boson) statistics. T_X is identical with the ambient neutrino temperature T_ν for X -particles that dominantly couple to neutrinos, while $T_X = T_\gamma$ for the electromagnetically coupled case. Since $y \geq x > 0$ and

$$(e^y \pm 1)^{-1} = e^{-y} \sum_{n=0}^{\infty} (\mp 1)^n e^{-ny} \quad (2)$$

we may expand the thermal integrals as

$$\begin{aligned} \int_x^\infty dy \frac{y(y^2 - x^2)^{1/2}}{e^y \pm 1} &= x^2 \sum_{n=0}^{\infty} (\mp 1)^n \frac{K_2[(1+n)x]}{1+n}, \\ \int_x^\infty dy \frac{(y^2 - x^2)^{3/2}}{e^y \pm 1} &= 3x^2 \sum_{n=0}^{\infty} (\mp 1)^n \frac{K_2[(1+n)x]}{(1+n)^2}, \\ \int_x^\infty dy \frac{y^2(y^2 - x^2)^{1/2}}{e^y \pm 1} &= \int_x^\infty dy \frac{(y^2 - x^2)^{3/2}}{e^y \pm 1} + x^2 \int_x^\infty dy \frac{(y^2 - x^2)^{1/2}}{e^y \pm 1} \\ &= \sum_{n=0}^{\infty} (\mp 1)^n \left(3x^2 \frac{K_2[(1+n)x]}{(1+n)^2} + x^3 \frac{K_1[(1+n)x]}{1+n} \right), \end{aligned} \quad (3)$$

where $K_l(x)$ is the special Bessel function of order l . In the numerical code the series are truncated at $n = 4$. The error of the physical quantities is always $\leq 0.18\%$.

A more subtle effect is caused by the conservation of entropy that implies a modified relation between the neutrino temperature T_ν and that of the electromagnetic plasma $T \equiv T_\gamma$. The cosmic entropy density is

$$s = \frac{2\pi^2}{45} g_{s*} T^3 = \frac{2\pi^2}{45} T^3 \sum_i g_{s*}^i, \quad (4)$$

where

$$\begin{aligned} g_{s*}^i(T) &= \frac{2\pi^2}{45T^3} \frac{\rho_i + P_i}{T_i} \\ &= \left(\frac{T_i}{T} \right)^3 \left(\sum_{\text{bosons}} g_i + \frac{7}{8} \sum_{\text{fermions}} g_i \right). \end{aligned} \quad (5)$$

The second equality applies for relativistic species, i.e. in the absence of warm species where $m \sim T$. Note that g_{s*}^i is always considered as a function of the temperature T of the electromagnetic plasma, not of T_i (a different notation is used in Ref. [13]). After neutrino decoupling at $T_D \approx 2.3$ MeV [16], the entropy in a comoving volume is separately conserved for the ‘‘neutrino plasma’’ and the electromagnetic one so that

$$\left[\frac{g_{s*}^\nu(T_D) g_{s*}^\gamma(T)}{g_{s*}^\nu(T) g_{s*}^\gamma(T_D)} \right]^{1/3} = 1. \quad (6)$$

For new particles being only electromagnetically coupled this equation simplifies to

$$\frac{T}{T_\nu} = \left[\frac{g_{s*}^\gamma(T_D)}{g_{s*}^\gamma(T)} \right]^{1/3}, \quad (7)$$

thus giving a higher temperature ratio relative to the standard case. This simulates the effect of $N_{\text{eff}} < 3$ thermally excited neutrino species at BBN and thus a reduced primordial helium abundance. The opposite is true for ν -coupled new particles.

The modified $T_\nu(T)$ relation also affects the $n \leftrightarrow p$ weak rates that depend on both T and T_ν through the phase-space dependence of the initial and final states of the processes. We implemented the modification of these rates in a perturbative way by introducing the small parameter

$$\delta(T) = \frac{T_\nu^0(T) - T_\nu(T)}{T_\nu(T)}, \quad (8)$$

where $T_\nu^0(T)$ is the standard dependence on the electromagnetic temperature T . Typically δ assumes values of order 0.01 and is always smaller than about 0.1. The neutrino temperature enters the weak rates through Fermi factors of the kind

$$\frac{1}{1 + \exp(az_\nu)}, \quad (9)$$

where $z_\nu = m_e/T_\nu$. Therefore, the additional terms for the rates can be obtained by integrating the factors

$$\frac{1}{1 + \exp[az_\nu^0(1 + \delta)]} - \frac{1}{1 + \exp(az_\nu^0)} = \sum_{n=1}^{\infty} f_n(az_\nu^0) \delta^n, \quad (10)$$

where in our numerical treatment the series was truncated to the third term. The corrections and the standard rates in the Born approximation were used to compute numerically the relative changes to the rates. Therefore, in the limit $\delta \rightarrow 0$ one recovers the $n \leftrightarrow p$ rates including finite mass, QED radiative and thermodynamic corrections, while disregarding modifications of these subleading effects in the $\delta \neq 0$ corrections. We finish with six functions $\epsilon_i(T)$

$$\begin{aligned} \frac{\Delta\Gamma_{n \rightarrow p}}{\Gamma_{n \rightarrow p}^0} &= \epsilon_{n1}(T)\delta + \epsilon_{n2}(T)\delta^2 + \epsilon_{n3}(T)\delta^3, \\ \frac{\Delta\Gamma_{p \rightarrow n}}{\Gamma_{p \rightarrow n}^0} &= \epsilon_{p1}(T)\delta + \epsilon_{p2}(T)\delta^2 + \epsilon_{p3}(T)\delta^3, \end{aligned} \quad (11)$$

fitting the change in the weak rates with an accuracy better than 5%.

In principle, one has a single covariant energy conservation equation for all components of the primordial plasma. For the sake of simplicity, however, in the previous considerations the ‘‘two fluids entropy conservation’’ was used to obtain the $T_\nu(T)$ relation. We can now derive the evolution of the thermodynamical quantities by applying the covariant energy conservation law to one of the two plasmas, e.g. the electromagnetic one, so that the first Friedmann equation is

$$\frac{dT}{dt} = -3H(\rho_{\text{em}} + P_{\text{em}}) \left(\frac{d\rho_{\text{em}}}{dT} \right)^{-1}, \quad (12)$$

where H depends on ρ_{tot} through the second Friedmann equation. If the additional species X couples to the electromagnetic fluid, the T - t -relation is further affected by a modified $(\rho_{\text{em}} + P_{\text{em}})$ factor, at least until the scattering freeze-out is reached. This has been roughly estimated to happen at $T \sim 35$ keV (Appendix B). In the numerical code, the X -particles were considered to decouple instantaneously from the electromagnetic component of the plasma for $T \leq 35$ keV. Relaxing this assumption our results remain essentially unchanged because for such low temperatures nucleosynthesis has almost completely stopped and the X -particles have a negligible impact, at least for the interesting mass range.

Another input parameter for the BBN calculation is the radiation density contributed by ordinary neutrinos which we fix to $N_{\text{eff}} = 3$.

Finally, we need the cosmic baryon density. The best-fit value from the temperature fluctuations of the cosmic microwave radiation as measured by the WMAP satellite is $\Omega_{\text{B}}h^2 = 0.024 \pm 0.001$ [17]. Including large-scale structure data from the 2dF galaxy redshift survey shifts this result to $\Omega_{\text{B}}h^2 = 0.023 \pm 0.001$, and including Lyman- α

data further shifts it to 0.0226 ± 0.0008 [17]. In our study we always use a fixed value of

$$\Omega_{\text{B}}h^2 = 0.023. \quad (13)$$

We have checked that for 2σ variations of $\Omega_{\text{B}}h^2$ our conclusions remain essentially unchanged. Note that in our BBN code the final value of $\eta \equiv n_{\text{B}}/n_\gamma$ or of $\Omega_{\text{B}}h^2$ is used to work out the one that enters the initial condition of the problem. We have

$$\eta_{\text{i}} = \frac{n_{\text{B}}^{\text{i}}}{n_\gamma^{\text{i}}} = \frac{n_{\text{B}}^{\text{f}} n_\gamma^{\text{f}} n_{\text{B}}^{\text{i}}}{n_\gamma^{\text{f}} n_\gamma^{\text{i}} n_{\text{B}}^{\text{f}}} = \eta_{\text{f}} \left(\frac{a_{\text{f}} T_{\text{f}}}{a_{\text{i}} T_{\text{i}}} \right)^3 \quad (14)$$

so that entropy conservation implies the well-known factor 11/4 in the standard case. In general it is a factor depending on the X -particle properties and was numerically evaluated.

B. Neutrino-Coupled Particles

As a first generic type of X -particles we consider particles that annihilate predominantly into neutrinos $X\bar{X} \leftrightarrow \nu\bar{\nu}$. We explicitly study three cases, that of Majorana fermions with a total of $g_X = 2$ inner degrees of freedom (case F2), self-conjugate scalar bosons with $g_X = 1$ (case B1), and scalar bosons with a particle and anti-particle degree of freedom ($g_X = 2$, case B2). With the ingredients discussed in the previous section we calculated the abundances for the light elements ${}^2\text{H}$, ${}^4\text{He}$, and ${}^7\text{Li}$ shown in Fig. 1 as a function of the new particle mass m_X . For $m_X \gtrsim 20$ MeV we recover the standard BBN predictions. For very small masses $m_X \rightarrow 0$ these particles freeze out relativistically and their effect on BBN is exactly that of $\Delta N_{\text{eff}} = 4/7$, 1, or $8/7$ additional relativistic neutrinos for the three cases B1, F2 and B2, as summarized in Table I.

The BBN effect of the new particles is dominated by their contribution to the primordial energy density and thus similar to an additional neutrino species. However, it is worthwhile to note the extra effect for intermediate m_X relative to the asymptotic case $m_X \rightarrow 0$. It is caused by the modified T_ν/T ratio previously described.

Our results essentially agree, both qualitatively and quantitatively, with those of Ref. [13], except for lithium. The difference is explained by our value of $\Omega_{\text{B}}h^2$ where the dependence of ${}^7\text{Li}$ on N_{eff} is opposite from the situation in Ref. [13]. In our case this nuclide is essentially produced through the channel ${}^4\text{He}({}^3\text{He}, \gamma){}^7\text{Be}(e^-, \nu_e){}^7\text{Li}$

TABLE I: Cases for new particles

Case		g_X	ΔN_{eff}	$\eta_{\text{i}}/\eta_{\text{f}}$
B1	Self-conjugate scalar boson	1	4/7	3.25
B2	Scalar boson $X \neq \bar{X}$	2	8/7	3.75
F2	Majorana fermion	2	1	3.65

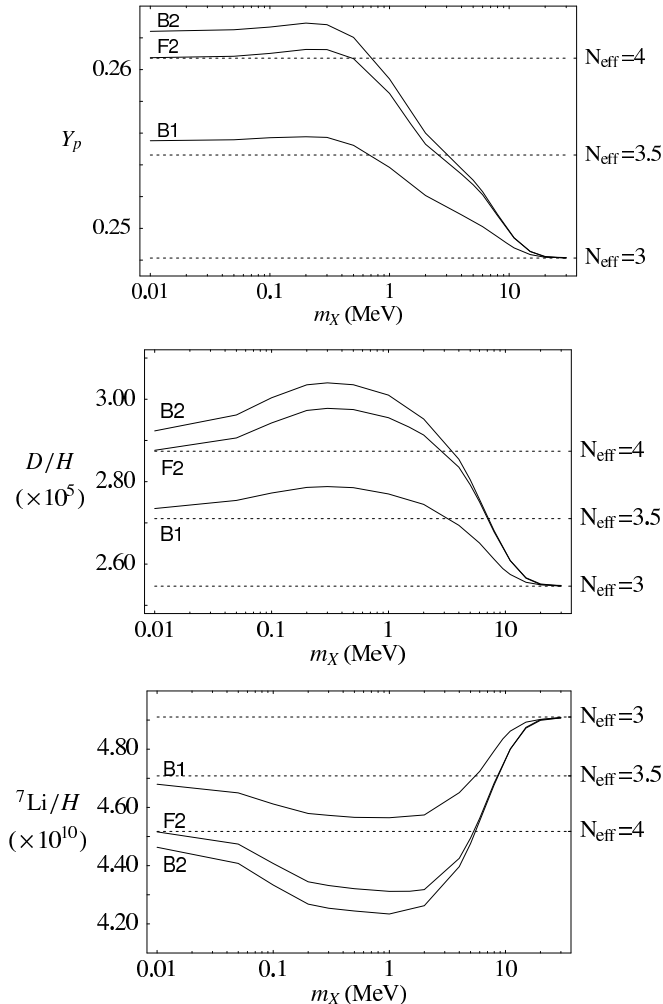


FIG. 1: Calculated light-element abundances for ${}^4\text{He}$ (top), ${}^2\text{H}$ (middle), and ${}^7\text{Li}$ (bottom) for neutrino-coupled new particles. The indicated cases B1, B2, and F2 are described in Table I. The horizontal lines indicate the effect of $N_{\text{eff}} = 3$, 3.5, and 4 relativistic neutrinos.

while at the lower value of $\Omega_B h^2$ used in Ref. [13] the direct channel ${}^4\text{He}({}^3\text{H}, \gamma){}^7\text{Li}$ dominates.

Our theoretical predictions can be compared with the measured primordial abundances summarized in Table II. For helium, the standard BBN prediction significantly exceeds the most recent measured value [19], and this discrepancy is even worse for other helium determinations that are lower (for a review see, e.g. Ref. [18]). Therefore, while different observations of the primordial ${}^4\text{He}$ abundance disagree on its exact value, a tension with the BBN prediction always exists. Our new particles exacerbate this discrepancy for $m_X \lesssim 10$ MeV and are thus disfavored or even excluded.

The deuterium abundance extracted from the QSO systems agrees perfectly with the BBN prediction, although it could be affected by possibly underestimated systematic errors. In any event, the new particles change the prediction only within the 1σ observational range so

TABLE II: Measured primordial light-element abundances

Element	Abundance	Reference
Helium ^a	${}^4\text{He}$ $Y_p = 0.2421 \pm 0.0021$	[19]
Deuterium	${}^2\text{H}$ $D/H = 2.78_{-0.38}^{+0.44} \times 10^{-5}$	[20]
Lithium	${}^7\text{Li}$ ${}^7\text{Li}/H = (1.70 \pm 0.17) \times 10^{-10}$	Refs. in [15]

^aFor other determinations and a short review, see also [18].

that deuterium adds little new information on the viability of the new particles.

A clear interpretation of the Spite plateau in the lithium data from metal-poor halo stars is still lacking so that it is not clear how to compare the lithium observations (average value given in Table II) with the theoretical prediction that is roughly a factor 2–3 larger. Both standard and non-standard physics explanations of this discrepancy have been invoked, e.g. Ref. [21] and references. Therefore, a meaningful comparison of our non-standard BBN prediction for lithium with observations is difficult. We show these results primarily for the purpose of illustration.

C. Electromagnetic Couplings

We next turn to new particles that do not interact with neutrinos but remain in perfect thermal equilibrium with the electromagnetic plasma throughout the BBN epoch by virtue of processes such as $X\bar{X} \leftrightarrow e^+e^-$ and $X + e \leftrightarrow X + e$. The BBN impact of these particles is more subtle and can be opposite to the neutrino-coupled case. Moreover, this is the case relevant as a source for galactic positrons [1, 2, 3, 4, 5]. For particles of this sort, there is a tension between the required primordial annihilation cross section to achieve the correct dark-matter density and the one in the galaxy to avoid overproducing positrons. The solution preferred in Refs. [1, 2, 3, 4, 5] is that of a predominant p-wave annihilation channel that will suppress the annihilation rate in the galaxy relative to that in the early universe. In particular, a specific model for a new boson was constructed where particles and anti-particles are not identical, i.e. our case B2. Of course, the detailed form of the cross section is not relevant for our work because we assume that the new particles are in perfect equilibrium with the electromagnetic plasma.

The calculated light-element abundances as functions of m_X are shown in Fig. 2. For $m_X \lesssim 2$ MeV the abundances are all shifted away from the observed values. However, for $m_X \gtrsim 2$ MeV the “entropy effect” works in the direction of lowering Y_p , by up to $\Delta Y_p \approx -0.002$ for the B2 case, without significantly affecting the ${}^2\text{H}$ and ${}^7\text{Li}$ predictions. Therefore, the concordance with the ${}^4\text{He}$ observations is improved. This point is illustrated more directly by Fig. 3 where we compare the new ${}^4\text{He}$ predictions for the cases B1 and B2 with the standard $N_{\text{eff}} = 3$

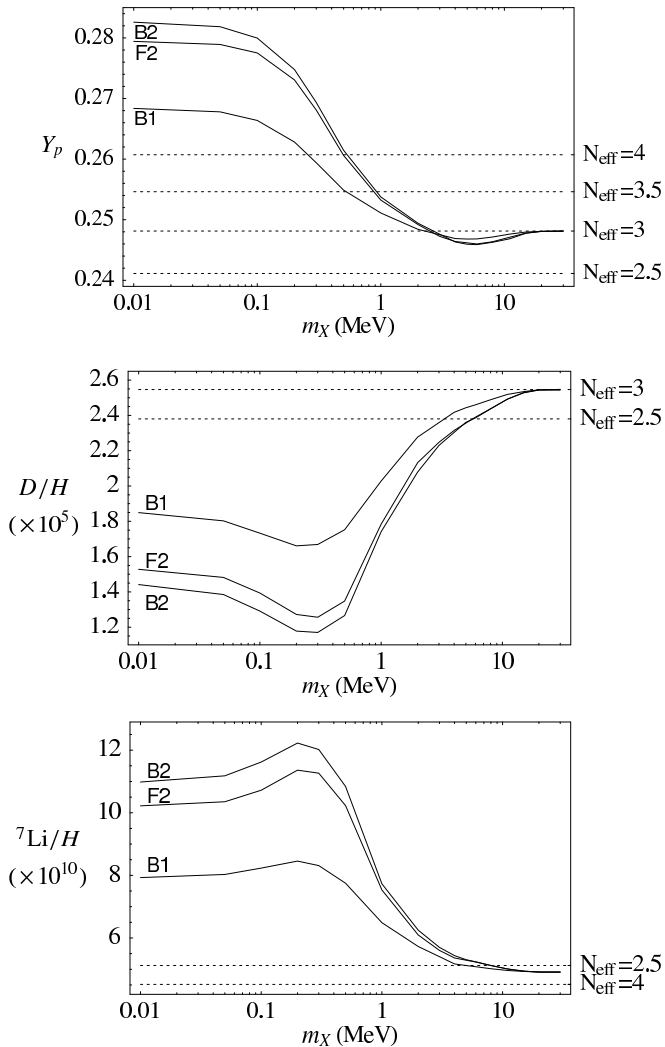


FIG. 2: Calculated light-element abundances for ${}^4\text{He}$ (top), ${}^2\text{H}$ (middle), and ${}^7\text{Li}$ (bottom) for electromagnetically coupled new particles. The indicated cases B1, B2, and F2 are described in Table I. The horizontal dotted lines indicate the standard predictions for the indicated values of the effective number of relativistic neutrino species, N_{eff} .

case and with the recent observational determination [19] for which the 1σ error band is shown. Y_p would benefit from this effect up to $m_X \lesssim 15$ MeV, even if the values $m_X \lesssim 10$ MeV are preferred. Our results again agree qualitatively with those of Ref. [13].

For low masses, the value of η_i needed to match the WMAP finding for η_f is significantly increased relative to the standard factor 2.75, as shown in the last column of Table I. This explains physically the huge decrease (increase) in the ${}^2\text{H}$ (${}^7\text{Li}$) yield that does not strongly depend on N_{eff} . Quite on the contrary, as Y_p depends only logarithmically on η , its change is essentially dominated by the addition of extra degrees of freedom to the electromagnetic plasma. The X -particles are now hotter than in the neutrino case and thus provoke a bigger effect. For $m_X \gtrsim 20$ MeV one recovers the standard predictions.

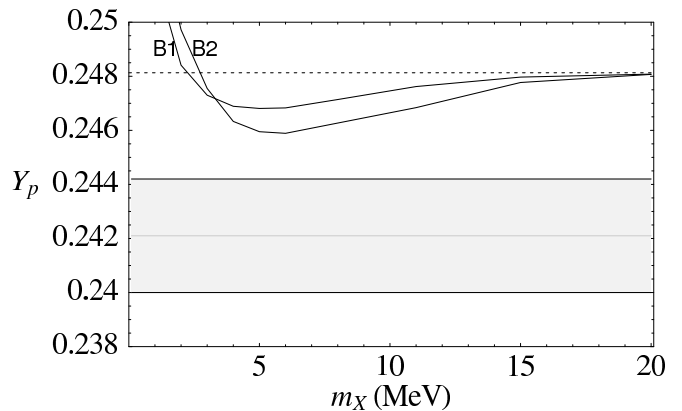


FIG. 3: ${}^4\text{He}$ abundance as in Fig. 2, here on a linear scale for m_X . The horizontal dotted line indicates the standard prediction for $N_{\text{eff}} = 3$. The gray band is the 1σ observational range for Y_p according to Ref. [19].

We have always neglected the role of dark matter residual annihilations during the freeze-out epoch. A detailed treatment of such effects is beyond the scope of our paper. However, an approximate study of this phenomenon (Appendix C) indicates that this late-time entropy generation effect is sub-dominant. Its effect goes in the direction of a further marginal reduction of Y_p and a small increase in the deuterium yield.

We have also neglected the possible photo-dissociation of ${}^2\text{H}$ and ${}^7\text{Li}$ induced by late dark matter annihilations. As shown in Appendix D, this effect is marginal unless, perhaps, if the dark matter particles couple directly with photons.

D. Particles Coupled both to the Electromagnetic Plasma and to Neutrinos

It may also be that the new particles interact strongly enough with both charged leptons and neutrinos to keep the two fluids in equilibrium beyond the usual decoupling epoch, a situation that was not previously treated. In this case $T_\gamma = T_\nu$ is maintained longer and perhaps throughout the nucleosynthesis epoch, depending on the new particle properties. This effect would be present even for very high m_X if one introduces an additional direct coupling of the neutrinos to the charged leptons through an extra gauge boson as in the preferred U -boson model discussed in Refs. [1, 2, 3, 4, 5]. Of course, in this case laboratory data, e.g. from ν - e scattering [22, 23], provide strong limits so that this situation may be rather unphysical.

In Fig. 4 we show the light-element abundances as a function of the assumed neutrino decoupling temperature T_D . If it is lowered to values $T_D \lesssim m_e$, the resulting modification of the light-element abundances is quite extreme and strictly excluded. For ${}^2\text{H}$ and ${}^7\text{Li}$ the “eta-effect” dominates, while for ${}^4\text{He}$ the change in T_ν/T and that of

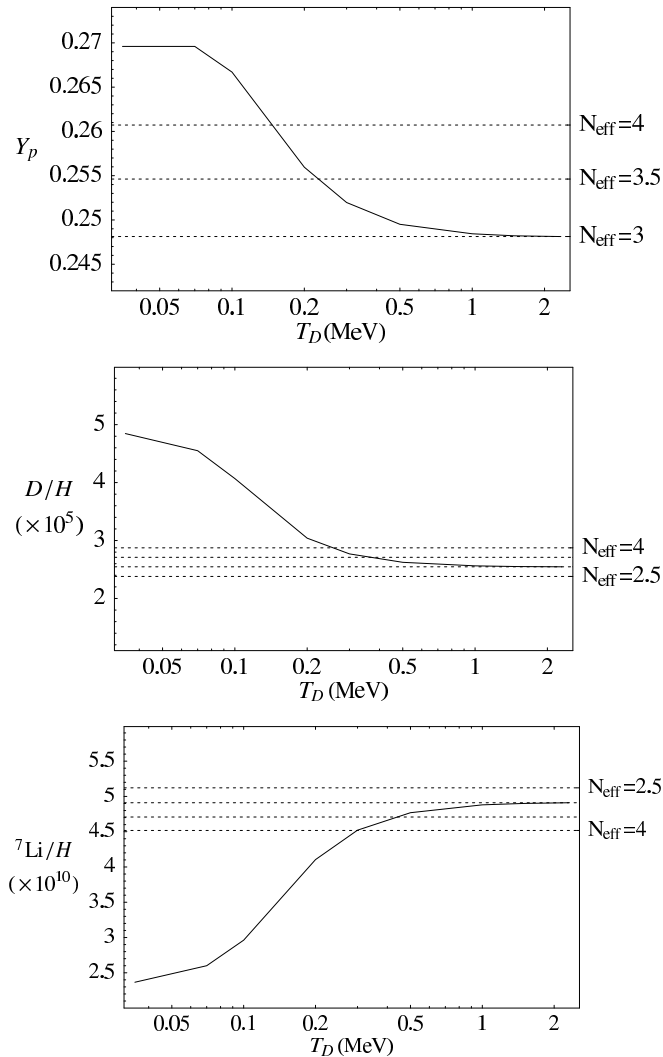


FIG. 4: Calculated light-element abundances for ${}^4\text{He}$ (top), ${}^2\text{H}$ (middle), and ${}^7\text{Li}$ (bottom) if the neutrino and electromagnetic plasmas are thermally coupled by a new interaction channel down to a temperature T_D . The horizontal lines indicate the standard predictions for the indicated values of the effective number of relativistic neutrino species, N_{eff} .

ρ_ν play a major role.

If the neutrinos and electromagnetic fluids are only indirectly coupled by their interactions with the new X -particles, the limiting condition to prolong the ν -equilibrium with the photon bath is the number density factor of the dark matter, n_X , in addition to the interaction cross sections. Qualitatively, we expect that for $m_X \lesssim m_e$ the combined effects conspire to hugely increase the ${}^4\text{He}$ yield, while some compensation could appear in the ${}^2\text{H}$ and ${}^7\text{Li}$ behavior. Obviously, for $m_X \gtrsim 20$ MeV one should recover the standard predictions, unless a direct ν - e coupling exists. A detailed kinetic study of this case would require a concrete particle physics model and is beyond the scope of our work.

III. LOW-ENERGY COSMIC RAY POSITRONS

The proposed MeV-mass dark matter particles discussed in Refs. [1, 2, 3, 4, 5] are supposed to annihilate in the galactic bulge and produce a flux of low-energy cosmic-ray positrons that can explain the observed 511 keV γ -ray signature. For such X -particles we also expect a flux of low-energy positrons at Earth from local dark-matter annihilation. Such a signature was already proposed for the detection of the traditional GeV–TeV mass range of dark matter particle candidates [24, 25]. For the case of annihilating MeV-mass dark matter particles we expect a much larger positron flux and therefore we study if additional constraints arise from the low-energy cosmic-ray positrons in the solar neighborhood.

To this end we derive the expected positron flux from X -particle annihilation. For a stationary situation the continuity equation for the cosmic-ray positrons is

$$q(E) - \frac{n(E)}{\tau(E)} + \frac{d[b(E)n(E)]}{dE} = 0, \quad (15)$$

where $n(E)$ is the differential positron density, $q(E)$ the injection spectrum, $\tau(E)$ an effective containment time, and $b(E) \equiv -dE/dt$ the energy-loss function. This equation is solved by

$$n(E) = \frac{1}{b(E)} \int_E^\infty ds q(s) \exp\left(-\int_E^s \frac{dy}{\tau(y)b(y)}\right). \quad (16)$$

The expected positron flux at the top of the atmosphere, neglecting solar modulation effects, is $j_{e^+} = n(E)/4\pi$, where we have assumed relativistic velocities.

In the relevant energy range and for an essentially neutral environment, ionization and bremsstrahlung are the dominant energy-loss mechanisms so that we have [26]

$$\begin{aligned} b(E) &\approx 36.18 m_e \sigma_T n_H \left[1 + 0.146 \ln\left(\frac{E}{m_e}\right) + \frac{E}{709 m_e} \right] \\ &= 3.69 \times 10^{-13} \text{ MeV s}^{-1} n_H [\dots]. \end{aligned} \quad (17)$$

Here, σ_T is the Thomson cross section and n_H the hydrogen density that dominates the interstellar medium. For the relevant energies, $b(E)$ is a slowly varying function.

It is easy to estimate that low-energy positrons do not travel far before annihilating so that the containment time $\tau(E)$ is identical with the annihilation time scale. The latter can be written in the form [27]

$$\tau(E) = \frac{1.33 \times 10^{14} \text{ s}}{f(E) n_H}, \quad (18)$$

where $f(E) = 0.02$ – 1 in the energy range of interest.

Finally we need the positron injection spectrum from dark-matter annihilation,

$$q(E) = n_X^2 \langle \sigma_a v \rangle \delta(1 - E/m_X), \quad (19)$$

where we have assumed that the X -particles are different from their antiparticles and that $n_X = n_{\bar{X}}$.

Equation (16) cannot be expressed in closed form, but for our purposes an analytical approximation is accurate enough. The factor $b\tau$ does not depend on n_H and is found to be

$$b\tau = 50\text{--}5000 \text{ MeV}, \quad (20)$$

where the range reflects the monotonic energy dependence. Ignoring this energy-dependence allows us to write the solution of Eq. (16) for $E \leq m_X$ as

$$n(E) \approx \frac{n_X^2 \langle \sigma_a v \rangle}{b(E)} \exp\left(-\frac{m_X - E}{b\tau}\right). \quad (21)$$

For the interesting range of m_X and E the exponential factor is always close to 1. Physically this represents the fact that positrons produced at energy $E = m_X$ will be lost from this “energy bin” primarily by down-scattering, not by annihilation.

In order to predict the positron flux we use $n_H = 1 \text{ cm}^{-3}$. For the local dark matter density we use the canonical value $\rho_{\text{DM}} = 300 \text{ MeV cm}^{-3} = m_X(n_X + n_{\bar{X}})$. For the annihilation cross section we first consider an s-wave model with $\langle \sigma_a v \rangle = \sigma_0$ where σ_0 is fixed by the early-universe freeze-out calculation (Appendix A). We compare the flux prediction with the best 95% CL upper limits in the 20–90 MeV range that are given in Fig. 4 of Ref. [28]. At 20 MeV, the flux limit is approximately $1.2 \times 10^{-5} \text{ cm}^{-2} \text{ s}^{-1} \text{ sr}^{-1} \text{ MeV}^{-1}$, for 30 MeV it is 8.5×10^{-6} in these units, for 50 MeV it is 2.5×10^{-6} , and for 90 MeV it is 9×10^{-7} .

We find flux predictions exceeding these limits by factors $\gtrsim 500$. This implies that the annihilation cross section required in the early universe for reducing the particle density to the dark-matter level produces an unacceptably large local positron flux and is thus excluded for $m_X > 20 \text{ MeV}$. For smaller m_X we have no constraint. For a p-wave channel we do not obtain any limits because $\langle \sigma_a v^2 \rangle$ is strongly suppressed in the galaxy because of the small dark-matter velocities v of order 10^{-3} .

Therefore, we confirm the conclusion of Refs. [1, 2, 3, 4, 5] that an s-wave annihilation channel $X\bar{X} \rightarrow e^+e^-$ is not acceptable for thermal relics. However, our argument does not depend on the uncertain dark-matter profile of the galactic bulge.

IV. ENERGY TRANSFER IN STARS

New MeV-mass particles could play an important role in stars. For example, they would be thermally produced in the collapsed core of a supernova and could contribute to the energy loss or the transfer of energy in these systems [29]. However, the X -particles discussed here have stronger-than-weak interactions, implying that in a supernova these effects would be small compared to those of ordinary neutrinos. Therefore, even though the new

particles would be thermally excited in a supernova core, there are no obvious observational consequences.

In ordinary stars, and especially in our Sun, dark-matter particles will be trapped and contribute to the transfer of energy in potentially observable ways [30]. In the following we investigate if MeV-mass particles could be relevant in this context. The result is that for MeV-range masses the evaporation time is very short so that the steady-state abundance of X -particles in the Sun is too small to be important.

A simple estimate of the energy conduction by the new particles can be worked out in a one-zone model of the Sun [30]. One assumes that the dark-matter stationary distribution in the Sun is globally Maxwellian at a uniform temperature T_X , with its maximum density found at a scale radius r_X . Assuming that T_X is identical with the temperature at the solar center, and taking r_X to be of order the solar radius, the luminosity carried by the new particles is of order

$$\frac{L_X}{L_\odot} \sim \frac{10^{-42} N_X}{(\sigma_s/\text{pb}) \sqrt{m_X/\text{MeV}}}, \quad (22)$$

where N_X is the total number of X -particles trapped in the Sun and σ_s is the scattering cross section on electrons, taken to be comparable to the annihilation cross section as described in Appendix B. For particles even more weakly interacting, i.e. for $\sigma_s \ll \text{few pb}$, one enters the Knudsen regime where the effect of energy transfer is much smaller [31, 32].

The steady-state number of dark-matter particles collected by the Sun arises from an equilibrium between capture and evaporation, i.e. $N_X = A/P_e$ with A the number of particles captured per unit time and P_e the escape probability per unit time. We estimate the capture rate to be [33, 34]

$$A \sim 4.34 \frac{n_X G_N M_\odot R_\odot}{v_{\text{gal}}} \quad (23)$$

where $v_{\text{gal}} \approx 300 \text{ km s}^{-1}$ is the mean square velocity of the galactic dark matter near the orbit of the Sun and n_X its number density.

The escape probability P_e is physically the ratio of the fraction of particles in the “escape-tail” of their distribution to the typical time needed to repopulate it. A simple estimate is [30]

$$P_e \sim \frac{(v_f \delta v)^{3/2}}{G_N M_\odot} \sqrt{\frac{m_X v_f^2}{2T_X}} \exp\left(-\frac{m_X v_f^2}{2T_X}\right), \quad (24)$$

where v_f is the escape velocity from a typical position in the Sun. Near the solar center one has $v_f \sim (15.8 T_X/m_p)^{1/2}$ [34]. Further, $\delta v \sim v_s m_s/m_X$ where m_s and v_s refer to the scattered particles, electrons in our case, for which we assume a thermal velocity distribution so that $v_s = (3T_s/m_s)^{1/2}$ and we assume $T_s = T_X$.

Based on these simple estimates and using a simplified solar model we find $N_X \sim 10^{36} (\text{pb}/\sigma_s)$. Comparing this

result with Eq. (22) we conclude that the effect of the new particles is too small to be significant for the Sun. Of course, our estimate is rather crude considering that the escape lifetime of the dark matter particles is comparable to their orbital period.

V. SUMMARY AND CONCLUSIONS

We have analyzed some astrophysical and cosmological consequences of the intriguing possibility that the cosmic dark matter consists of MeV-mass particles [1, 2, 3, 4, 5]. These particles are assumed to be thermal relics and thus have interaction cross sections that are larger than weak.

Such particles do not have any apparent consequences for stellar evolution. In supernovae, their interaction is too strong so that neutrinos continue to play the leading role for energy loss and energy transfer. In the Sun, the particle mass is so small that evaporation prevents the trapped steady-state population from growing large enough for a significant contribution to energy conduction.

We have derived new constraints coming from the low-energy positron component of cosmic rays. An s-wave annihilation cross section for $X\bar{X} \rightarrow e^+e^-$ as large as implied by the early-universe freeze-out calculation causes an excessive positron flux for $m_X = 20\text{--}90$ MeV where experimental upper limits are available. Therefore, only p-wave annihilation is compatible with these constraints. These conclusions agree with those reached in Refs. [1, 2, 3, 4, 5], but in our case they do not depend on the assumed dark-matter profile of the galactic bulge.

The main subject of our work, however, was the impact of MeV-mass particles on big-bang nucleosynthesis (BBN). Significant modifications arise only for $m_X \lesssim 20$ MeV. The effects found are largely independent of the energy dependence of the annihilation cross section and even of its exact value, provided that it is high enough to take the new particles to equilibrium with the neutrinos or the electromagnetic plasma.

For the neutrino-coupled case, the impact of the new particles is comparable to that of additional neutrino species. Notably, the primordial helium abundance is increased, exacerbating the discrepancy between predictions and observations. Therefore, such X -particles are disfavored by BBN for masses up to about 10 MeV.

For the electromagnetically coupled case, the BBN concordance would be severely disturbed for $m_X \lesssim 2$ MeV. However, there is a region $m_X = 4\text{--}10$ MeV where the primordial helium mass fraction Y_p is actually reduced relative to the standard case while the predicted ^2H remains compatible with observations. This non-trivial phenomenon is a consequence of the “entropy effect” discussed in the paper. While this effect was already found in Ref. [13], it now assumes greater importance because it slightly improves the discrepancy between the BBN predictions for Y_p and its observed value.

In summary, the MeV-mass dark matter particles pro-

posed in Refs. [1, 2, 3, 4, 5] as a source for positrons in the galactic bulge are not incompatible with BBN, provided the particle mass exceeds a few MeV. On the contrary, in the mass range $m_X = 4\text{--}10$ MeV these particles slightly improve the concordance between BBN calculations and the observed helium abundance. It is quite fascinating that such exotic particles, far from being excluded, seem to have several beneficial consequences in astrophysics and cosmology.

Acknowledgments

In Munich, this work was supported in part by the Deutsche Forschungsgemeinschaft under grant SFB 375 and the ESF network Neutrino Astrophysics. We thank D. Semikoz, M. Kachelriess and the members of the Naples Astroparticle Group for useful discussions and comments.

APPENDIX A: RELIC DENSITY AND ANNIHILATION CROSS SECTION

Once the mass m_X and the spin multiplicity g_X of a thermal relic are fixed, the requirement that it is the dark matter uniquely determines the annihilation freeze-out temperature T_F and the annihilation reaction rate at this temperature $\langle\sigma_a v\rangle_{T_F}$. The relic mass density is

$$\Omega_X h^2 = \frac{8\pi h^2 m_X n_X}{3m_{\text{Pl}}^2 H^2} = \frac{8\pi m_X s}{3(m_{\text{Pl}} H/h)^2} \left(\frac{n_X}{s}\right), \quad (\text{A1})$$

where $H/h = 100 \text{ km s}^{-1} \text{ Mpc}^{-1}$, $m_{\text{Pl}} = 1.22 \times 10^{22}$ MeV is the Planck mass, and s is the entropy density. Note that for particles that are not self-conjugate Ω_X only includes the particles so that $\Omega_{\text{DM}} = \Omega_X + \Omega_{\bar{X}}$.

Neglecting entropy-producing phenomena, the entropy per comoving volume remains constant so that

$$\left(\frac{n_X}{s}\right)_0 = \left(\frac{n_X}{s}\right)_{T_F} \quad (\text{A2})$$

for $T \leq T_F$. If one assumes a functional form for $\langle\sigma_a v\rangle_T$, an order-of-magnitude estimate of T_F is given by the condition $n_X \langle\sigma v\rangle_{T_F} = H(T_F)$. A more accurate formula is obtained by a semi-analytical treatment of the Boltzmann equation [14]

$$x_F = x_0 - (n + \frac{1}{2}) \log x_0, \quad (\text{A3})$$

where

$$x_0 = \log \left[0.038 (n + 1) \frac{g_X}{\sqrt{g_{*F}}} m_{\text{Pl}} m_X \sigma_n \right]. \quad (\text{A4})$$

Here, the parameterization

$$\langle\sigma_a v\rangle_T = \sigma_n x^{-n} \quad (\text{A5})$$

with $x = m_X/T$ was assumed. The most interesting cases are obtained for $n = 0$ (s-wave annihilation) and $n = 1$ (p-wave). The previous equations yield

$$\begin{aligned} \left(\frac{n_X}{s}\right)_0 &= \frac{3.79 \sqrt{g_{*F}} (n+1) x_F^{n+1}}{g_{*F} m_{\text{Pl}} m_X \sigma_n}, \\ \Omega_X h^2 &= 0.032 \frac{(n+1) x_F^{n+1} \sqrt{g_{*F}}}{g_{*F} (\sigma_n/\text{pb})}, \end{aligned} \quad (\text{A6})$$

with an accuracy better than 5%. Since $\Omega_{\text{DM}} h^2 \approx 0.11$ [17], and $x_F = 15\text{--}20$, it is easily seen that, for $X \neq \bar{X}$, one has $\sigma_0 \sim 5$ pb and $\sigma_1 \sim 10^2$ pb.

APPENDIX B: KINETIC FREEZE-OUT

We estimate the kinetic freeze-out temperature for X -particles coupled to the electromagnetic plasma. We make the rough approximation that the annihilation and scattering cross sections are comparable, $\sigma_a \sim \sigma_s$, so that the ratio between the annihilation and scattering rates is essentially given by $\Gamma_a/\Gamma_s \sim n_X/n_s$. For our case the scattering targets are electrons and positrons so that

$$n_s = n_{e^+} + n_{e^-} = 4 \left(\frac{m_e^2}{2\pi z}\right)^{3/2} e^{-z} \cosh \xi_e, \quad (\text{B1})$$

where $\xi_e \equiv \mu_e/T$ is the electron degeneracy parameter and $z \equiv m_e/T$. Therefore, as long as the X -particles are in kinetic equilibrium we have

$$\frac{\Gamma_a}{\Gamma_s} \approx \frac{1}{2} \left(\frac{m_X}{m_e}\right)^{3/2} \exp\left(-\frac{m_X - m_e}{T}\right) \frac{1}{2 \cosh \xi_e} \quad (\text{B2})$$

This result applies at T_F only if $(\Gamma_a/\Gamma_s)_{T_F} \ll 1$. Assuming $m_X = 1$ MeV, one finds from Eq. (A3) that $T_F \approx 0.07$ MeV and from a standard BBN code that $\xi_e(T_F) \approx 0.32 \times 10^{-7}$ so that $(\Gamma_a/\Gamma_s)_{T_F} \approx 4 \times 10^{-4}$ which is indeed $\ll 1$.

Once a value for the annihilation effective cross section σ_n has been determined, one can easily deduce a kinetic freeze-out temperature T_K for the decoupling of the dark matter particles from the electromagnetic plasma, assuming that $\sigma_a \sim \sigma_s$. The condition $\Gamma_s(T_K) = H(T_K)$ implies

$$\langle \sigma_s v \rangle_{T_K} = \frac{5.44 T_K^2}{m_{\text{Pl}} n_s(T_K)} \sqrt{\frac{g_*(T_K)}{10.75}}. \quad (\text{B3})$$

With $\cosh \xi_e \approx 1$ and $g_* \approx 3.36$ one obtains

$$z_K - (0.5 - \ell) \log z_K \approx 14.1 + \log(\sigma_{s,\ell}/\text{pb}), \quad (\text{B4})$$

where $\langle \sigma_s v \rangle \equiv \sigma_{s,\ell} z^{-\ell}$. For typical values of $\sigma_{s,n}$ this gives $T_K \approx 35$ keV.

APPENDIX C: ENTROPY GENERATION DURING DECOUPLING

We sketch an argument that indicates that the entropy production associated with the dark-matter freeze-out is a sub-leading effect. To this end we assume that every e^+e^- annihilation product is instantaneously thermalized and converted into photons. In this case the evolution equation for the X number density is [14]

$$\dot{n}_X + 3Hn_X = -C[n_X] \quad (\text{C1})$$

where

$$C[n_X] = \langle \sigma_a v \rangle [n_X^2 - n_{X,\text{eq}}^2]. \quad (\text{C2})$$

The same equation applies to $n_{\bar{X}} = n_X$ because we always assume equal distributions for both X and \bar{X} . The subsequent e^+e^- annihilations imply

$$\dot{n}_\gamma + 3Hn_\gamma = +2C[n_X]. \quad (\text{C3})$$

The equilibrium energy densities are

$$\begin{aligned} \rho_\gamma &= \left(\frac{\pi^2}{15}\right) \left(\frac{\pi^2}{2\zeta(3)}\right)^{4/3} n_\gamma^{4/3}, \\ \rho_X &= n_X \left(m_X + \frac{3}{2}T\right), \end{aligned} \quad (\text{C4})$$

where the non-relativistic regime was used for the dark-matter particles. The energy injection by late annihilations is estimated as

$$\begin{aligned} \dot{\rho}_\gamma &= \frac{8}{3} \left(\frac{\pi^4 T}{30\zeta(3)}\right) C[n_X], \\ \dot{\rho}_X &= -m_X \left(1 + \frac{3T}{2m_X}\right) C[n_X]. \end{aligned} \quad (\text{C5})$$

The direct change of the total energy density due to this conversion of dark-matter particles into photons is a very small effect, as one can see by evaluating the ratios $\dot{\rho}_\gamma/\rho_\gamma$ and \dot{n}_γ/n_γ .

The main non-negligible consequence is on the T - t relation (first Friedmann equation) through the second term in the following equation

$$\begin{aligned} \frac{d\rho_{\text{em}}}{dt} &= -3H(\rho + P)_{\text{em}} \\ &\quad - \left[m_X - \left(\frac{4\pi^4}{45\zeta(3)} - 3\right) T \right] C[n_X]. \end{aligned} \quad (\text{C6})$$

The problem is then restricted to the solution of the equation for n_X in order to calculate the relevant quantity $C[n_X]$. This was done by standard techniques after some standard substitutions (see e.g. Ref. [14]). We found a negligible effect on Y_p , and a change of the ${}^2\text{H}$ and ${}^7\text{Li}$ yields of order 0.1 in the units of Fig. 2. Therefore, we are indeed dealing with a sub-leading effect.

APPENDIX D: DEUTERIUM PHOTO-DISSOCIATION

We show that the dissociation of fragile nuclides, principally deuterium, by late dark-matter annihilation is completely negligible. To this end we first follow standard works on this subject (e.g. Ref. [35]) and note that the “first-generation” of nonthermal photons is rapidly degraded to have a spectrum with a high energy cut $E_C \approx m_e^2/22T$ because of the highly efficient pair creation and subsequent reactions on the background medium. This means that in order for some photons to survive and to be able to dissociate nuclei the temperature has to drop at least to values $T \lesssim m_e^2/22B_D \approx 5$ keV, where $B_D \approx 2.2$ MeV is the binding energy of deuterium. This implies that neglecting this phenomenon during the BBN epoch is certainly a good approximation. Note also that in our preferred models, MeV-mass X particles would not annihilate directly into photons, so the “first-generation” photon spectrum is already degraded in energy because it is produced by secondary effects of the primary electrons and positrons.

Therefore, by simply looking at the expected energy spectrum, the most dangerous process would be the electro-disintegration of deuterium, for which a further 0.5 MeV penalty in the energy should be considered as the electron rest mass would not be released. Without invoking a detailed analysis we conclude that our results up to $m_X \lesssim 2.7$ MeV remain unchanged.

For higher values of m_X considered in our BBN analysis, say 3–20 MeV, we reach the same conclusion by following the treatment of the late-time annihilations of a relic particle described in Ref. [36]. Assuming that electro-dissociation of deuterium is the only relevant phenomenon, the D depletion factor can be written as

$$\exp \left[- \int_{t_i}^{t_f} dt \Gamma_{eD}(t) \right], \quad (D1)$$

where t_i is the time at the onset of dissociation, t_f is some late time where the D abundance is observed, and

$$\Gamma_{eD} = s \int_{B_D}^{E_C(T)} dE f_e(E, T) \sigma_{eD}(E). \quad (D2)$$

Here, $\sigma_{eD}(E) \approx 13.3 \mu\text{b} [(E - B_D)/\text{MeV}]^{1/2}$ is the electro-dissociation cross-section of deuterium [37]. Further, $f_e(E, T)$ is the “steady state” dark-matter annihilation product spectrum. By arguments similar to the ones presented in Ref. [36] it is written as

$$f_e(E, T) \approx \sigma_n \left(\frac{T}{m_X} \right)^n \frac{s}{n_\gamma \sigma_{e\gamma}(E)} \left(\frac{n_X}{s} \right)^2 \times \frac{m_X \theta[E_{\max}(T) - E]}{\sqrt{E^3 E_C(T)}}, \quad (D3)$$

where $\sigma_{e\gamma}(E)$ is the Compton scattering cross section and $E_{\max}(T) = \text{Min}[E_C(T), m_X]$. Note that the primary particle’s “first” shower spectrum has roughly the same shape for γ or e initiated showers [35, 36].

We have numerically solved the integral in Eq. (D1) by changing to the temperature variable and assuming a radiation dominated universe. The effects we found are completely negligible both for s- and p-wave annihilations.

Note, however, that for showers induced by secondary photons one should replace in Eq. (D3) the huge factor n_γ with n_e , and the electro-dissociation cross section with the photo-dissociation one, while a penalty factor in the energy spectrum would enter. Making some extreme assumption one could thus gain up to a factor 10^{12} of the previous estimates. Even so, it is not enough to affect by more than a few percent our simplified nuclides’ predictions. The effects are even less pronounced for the preferred case $n = 1$ (p-wave annihilation).

-
- [1] C. Boehm, T. A. Ensslin and J. Silk, “Are light annihilating dark matter particles possible?,” *J. Phys. G* **30**, 279 (2004) [astro-ph/0208458].
 - [2] C. Boehm and P. Fayet, “Scalar dark matter candidates,” *Nucl. Phys. B* **683**, 219 (2004) [hep-ph/0305261].
 - [3] C. Boehm, D. Hooper, J. Silk and M. Casse, *Phys. Rev. Lett.* **92** (2004) 101301 [arXiv:astro-ph/0309686].
 - [4] D. Hooper, F. Ferrer, C. Boehm, J. Silk, J. Paul, N. W. Evans and M. Casse, “MeV dark matter in dwarf spheroidals: A smoking gun?,” astro-ph/0311150.
 - [5] C. Boehm, P. Fayet and J. Silk, “Light and heavy dark matter particles,” hep-ph/0311143.
 - [6] K. Abazajian, G. M. Fuller and M. Patel, “Sterile neutrino hot, warm, and cold dark matter,” *Phys. Rev. D* **64**, 023501 (2001) [astro-ph/0101524].
 - [7] L. Covi, L. Roszkowski and M. Small, “Effects of squark processes on the axino CDM abundance,” *JHEP* **0207**, 023 (2002) [hep-ph/0206119].
 - [8] C. Bird, P. Jackson, R. Kowalewski and M. Pospelov, “Search for dark matter in $b \rightarrow s$ transitions with missing energy,” [hep-ph/0401195] state that a light scalar dark matter candidate is excluded, based on $b \rightarrow s$ transitions with missing energy. However, they assume a coupling with the Standard Model particles through the Higgs sector, in contrast with the more exotic models discussed in [1, 2, 3, 4, 5].
 - [9] P. Jean *et al.*, “Early SPI/INTEGRAL measurements of galactic 511 keV line emission from positron annihilation,” *Astron. Astrophys.* **407**, L55 (2003) [astro-ph/0309484].
 - [10] J. Knodlseder *et al.*, “Early SPI/INTEGRAL constraints on the morphology of the 511 keV line emission in the 4th galactic quadrant,” astro-ph/0309442, accepted for publication in *Astron. Astrophys.*
 - [11] C. Picciotto and M. Pospelov, “Unstable Relics as a Source of Galactic Positrons,” hep-ph/0402178.

- [12] D. Hooper and L. T. Wang, “Evidence for axino dark matter in the galactic bulge,” hep-ph/0402220.
- [13] E. W. Kolb, M. S. Turner and T. P. Walker, “The effect of interacting particles on primordial nucleosynthesis,” Phys. Rev. D **34**, 2197 (1986).
- [14] E. W. Kolb and M. S. Turner, *The Early Universe* (Addison-Wesley, Redwood City, CA, 1989).
- [15] A. Cuoco, F. Iocco, G. Mangano, G. Miele, O. Pisanti and P. D. Serpico, “Present status of primordial nucleosynthesis after WMAP: Results from a new BBN code,” to be published in Int.J.Mod.Phys.A [astro-ph/0307213].
- [16] K. Enqvist, K. Kainulainen and V. Semikoz, “Neutrino annihilation in hot plasma,” Nucl. Phys. B **374**, 392 (1992).
- [17] D. N. Spergel *et al.*, “First Year Wilkinson Microwave Anisotropy Probe (WMAP) Observations: Determination of cosmological parameters,” Astrophys. J. Suppl. **148**, 175 (2003) [astro-ph/0302209].
- [18] K. Hagiwara *et al.* [Particle Data Group Collaboration], “Review Of Particle Physics,” Phys. Rev. D **66** (2002) 010001.
- [19] Y. I. Izotov and T. X. Thuan, “Systematic effects and a new determination of the primordial abundance of ^4He and dY/dZ from observations of blue compact galaxies,” Astrophys. J. **602**, 200 (2004) [astro-ph/0310421].
- [20] D. Kirkman, D. Tytler, N. Suzuki, J. M. O’Meara and D. Lubin, “The cosmological baryon density from the deuterium to hydrogen ratio towards QSO absorption systems: D/H towards Q1243+3047,” Astrophys. J. Suppl. **149**, 1 (2003) [astro-ph/0302006].
- [21] K. Jedamzik, “Did something decay, evaporate, or annihilate during big bang nucleosynthesis?,” astro-ph/0402344.
- [22] R. C. Allen *et al.*, “Study of electron-neutrino electron elastic scattering at LAMPF,” Phys. Rev. D **47**, 11 (1993).
- [23] L. B. Auerbach *et al.* (LSND Collaboration), “Measurement of electron-neutrino electron elastic scattering,” Phys. Rev. D **63**, 112001 (2001) [hep-ex/0101039].
- [24] A. J. Tylka, “Cosmic ray positrons from annihilation of weakly interacting massive particles in the galaxy,” Phys. Rev. Lett. **63**, 840 (1989), Erratum *ibid.* **63**, 1658 (1989).
- [25] M. S. Turner and F. Wilczek, “Positron line radiation from halo WIMP annihilations as a dark matter signature,” Phys. Rev. D **42**, 1001 (1990).
- [26] R. Schlickeiser, *Cosmic Ray Astrophysics* (Springer, Berlin, 2002).
- [27] R. Svensson, “The pair annihilation process in relativistic plasmas,” Astrophys. J. **258**, 321 (1982).
- [28] R. C. Hartman and C. J. Pellerin, “Cosmic-ray positron and negatron spectra between 20 and 800 MeV measured in 1974,” Astrophys. J. **204**, 927 (1976).
- [29] G. G. Raffelt, “Particle physics from stars,” Ann. Rev. Nucl. Part. Sci. **49**, 163 (1999) [hep-ph/9903472].
- [30] D. N. Spergel and W. H. Press, “Effect of hypothetical, weakly interacting, massive particles on energy transport in the solar interior,” Astrophys. J. **294**, 663 (1985).
- [31] A. Gould and G. Raffelt, “Cosmion energy transfer in stars: The Knudsen limit,” Astrophys. J. **352**, 669 (1990).
- [32] A. Gould and G. Raffelt, “Thermal conduction by massive particles,” Astrophys. J. **352**, 654 (1990).
- [33] A. Gould, “Resonant enhancements in WIMP capture by the Earth,” Astrophys. J. **321**, 571 (1987).
- [34] W. H. Press and D. N. Spergel, “Capture by the Sun of a galactic population of weakly interacting, massive particles,” Astrophys. J. **296**, 679 (1985).
- [35] M. Kawasaki and T. Moroi, “Electromagnetic cascade in the early universe and its application to the big bang nucleosynthesis,” Astrophys. J. **452** (1995) 506 [arXiv:astro-ph/9412055].
- [36] J. A. Frieman, E. W. Kolb and M. S. Turner, “Eternal Annihilations: New Constraints On Longlived Particles From Big Bang Nucleosynthesis,” Phys. Rev. D **41** (1990) 3080.
- [37] H. S. Picker, “Electrodisintegration and electrocapture in primordial nucleosynthesis,” Phys. Rev. C **30** (1984) 1751.